

Extension of the Nyquist Robust Stability Margin to Systems with Nonconvex Value Sets

C. T. Baab
Department of Chemical Engineering
University of Florida
Gainesville, FL 32611-6005
baabct@che.ufl.edu

H. A. Latchman
Department of Electrical Engineering
University of Florida
Gainesville, FL 32611
latchman@list.ufl.edu

J. C. Cockburn
Department of Electrical Engineering
Florida A&M University – Florida State University
Tallahassee, FL 32310
cockburn@eng.fsu.edu

O. D. Crisalle *
Department of Chemical Engineering
University of Florida
Gainesville, FL 32611-6005
crisalle@che.ufl.edu

Abstract

The Nyquist robust stability margin is proposed as a measure of robust stability for systems with affine parametric uncertainty. The work extends the critical-direction theory to include nonconvex critical uncertainty value sets through the introduction of a more general definition of the critical perturbation radius. The approach is specialized to the case of real parametric affine uncertainty models, and it is shown that the critical perturbation radius can be calculated precisely using an explicit map from the parameter space to the Nyquist plane.

1. Introduction

The stability analysis of feedback control systems in the presence of modeling uncertainty is the subject of extensive studies; in particular, the class of structured uncertainties where the parameters of a transfer function vary in prescribed real intervals is relevant to many engineering applications. Early advances in this field are due to the well-known theorem by Kharitonov (1979) that gives conditions for the stability of polynomial systems with coefficients that belong to a rectangular polytope. Extensions of Kharitonov's work to rational functions make use of standard frequency-domain techniques such as Nyquist plots and the small gain theorem. These methods are based on determining the stability of a set of Kharitonov plants (or extreme plants) derived from an interval plant description where each coefficient of the numerator and denominator polynomial varies in a fixed interval. The number of extreme plants required varies with the technique utilized. Chapellat *et al.* (1989) suggest a method which involves checking the stability and calculating H_∞ norms along a finite number (at most 32) of extreme segments called Kharitonov segments. Barnish

et al. (1992) prove that it is necessary and sufficient that sixteen of the extreme plants be stable, and under certain conditions only eight or twelve are necessary. Bartlett *et al.* (1990) give conditions that use 32 one-dimensional subsets of the interval plant.

Available results for interval plant descriptions enable the development of computationally manageable methods for solving a wide range of robust stability analysis problems. However, it is usually the case that each plant coefficient depends on more than one uncertain parameter. One such uncertainty description occurs when the plant coefficients are affine in the uncertain parameters. Unfortunately, the extension of Kharitonov's approach to the case of affine uncertainties is not straightforward. Nevertheless, Fu (1990) presents comprehensive results that are useful for quantifying an entire uncertainty value set in the Nyquist plane for plants with affine parametric uncertainties. A remaining challenge is to utilize these results to produce a scalar measure of robustness analogous to the well known structured singular value (Doyle, 1982) and the multivariable stability margin (Safonov, 1982) paradigms.

This paper proposes an alternative method that is applicable to both interval and affine perturbations and is based on using the Nyquist robust stability margin $k_N(\omega)$ as a measure of robust stability. The technique extends the critical-direction theory developed by Latchman and Crisalle (1995) and Latchman *et al.* (1997) by considering nonconvex critical uncertainty value sets. A general definition of the critical perturbation radius $\rho_c(\omega)$ used in the calculation of $k_N(\omega)$ is proposed to take into account nonconvex critical uncertainty value sets. The new general theory is applied to the case of systems with real parametric affine uncertainties. Earlier results of Fu (1990) are combined with an explicit map from the

* Author to whom all correspondence should be addressed.

parameter space to the Nyquist plane to calculate the required critical perturbation radius with high precision and efficiency.

2. Preliminaries

Consider the single-input single-output system

$$g(s) = g_0(s) + \delta(s) \quad (1)$$

where $g_0(s)$ is a known nominal system and $\delta(s) \in \Delta$ represents a linear perturbation. The focus of this analysis is on the stability of the closed-loop system that results when the uncertain plant (1) is configured in the unity feedback control structure shown in Figure 1.

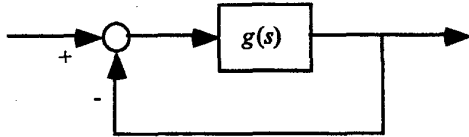


Figure 1. Uncertain plant feedback structure.

Under the standard assumption that Δ is such that $g(s)$ and $g_0(s)$ have the same number of open loop unstable poles, it then follows that the stability of the system can be assessed using the approach of Latchman and Crisalle (1995) and Latchman *et al.* (1997), a frequency-domain robustness analysis technique that makes use of several objects defined in the Nyquist plane as shown in Figure 2. Of particular importance are the *critical direction*

$$d_c(j\omega) := -\frac{1+g_0(j\omega)}{|1+g_0(j\omega)|}$$

which is interpreted as the unit vector from $g_0(s)$ to the critical point $-1+j0$, and the *critical line* $r(\omega) := g_0(j\omega) + \alpha d_c(j\omega)$, $\alpha \geq 0$, which is interpreted as the directed line (*i.e.*, a ray) which originates at the nominal point $g_0(s)$ and passes through the critical point $-1+j0$. The *uncertainty value set* (or template) $\mathcal{V}(\omega) := \{g(j\omega) \mid g(j\omega) = g_0(j\omega) + \delta(j\omega), \delta(s) \in \Delta\}$ is the image of $g(s)$ on the Nyquist plane, and the *critical uncertainty value Set* $\mathcal{V}_c(\omega) := \mathcal{V}(\omega) \cap r(\omega)$ is defined as the intersection of the uncertainty value set with the critical line. The *critical perturbation radius* is defined as

$$\rho_c(\omega) := \max_{\alpha \in \mathbb{R}^+} \{ \alpha \mid z = g_0(j\omega) + \alpha d_c(j\omega) \in \mathcal{V}(\omega) \} \quad (2)$$

for the case where $\mathcal{V}_c(\omega)$ is convex (Latchman *et al.*, 1997). In order to account for those cases where $\mathcal{V}_c(\omega)$ is nonconvex, we introduce the following new and general definition for the critical perturbation radius:

$$\rho_c(\omega) := \begin{cases} |1+g_0(j\omega)| - \xi(j\omega) & \text{if } -1 \notin \mathcal{V}_c(\omega) \\ |1+g_0(j\omega)| + \xi(j\omega) & \text{otherwise} \end{cases} \quad (3)$$

where

$$\xi(j\omega) := \min_{\alpha \in \mathbb{R}} \{ |\alpha| \mid z = -1 + \alpha d_c(j\omega) \in \mathcal{V}(\omega) \}$$

Finally, for either definition of the critical perturbation radius, the *Nyquist robust stability margin* is defined as

$$k_N(\omega) := \frac{\rho_c(\omega)}{|1+g_0(j\omega)|}$$

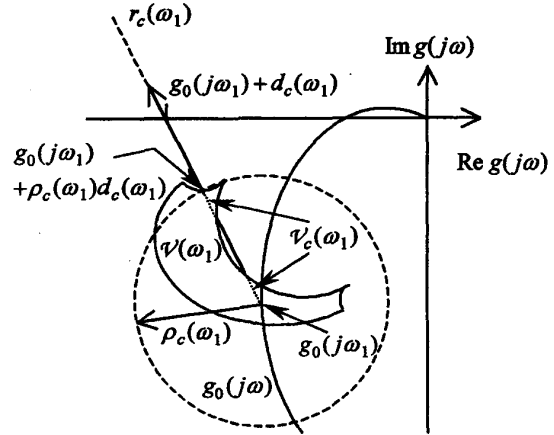


Figure 2. Typical uncertainty value set $\mathcal{V}(\omega_1)$ at frequency ω_1 and its critical perturbation radius $\rho_c(\omega_1)$. Also shown in the figure are the critical line $r(\omega_1)$ and the nonconvex critical uncertainty value set $\mathcal{V}_c(\omega_1)$.

From Figure 2 it follows that at each frequency ω the critical direction $d_c(j\omega)$ may be interpreted as a unit vector with origin at the nominal point $g_0(j\omega)$ and pointing towards the critical point $-1+j0$ on the Nyquist plane. The figure shows a nonconvex bounded uncertainty value set $\mathcal{V}(\omega)$. Also note the nonconvexity of the critical uncertainty value set, $\mathcal{V}_c(\omega)$, which is in fact the subset of $\mathcal{V}(\omega)$ that lies along the straight-line segment joining the nominal plant $g_0(j\omega)$ and the critical point $-1+j0$.

The main result of the critical direction theory is stated in the following theorem.

Theorem 2.1. Consider the uncertain system $g(s)$ given in (1) and suppose that the nominal system $g_0(s)$ is stable under unity feedback, and that $g(s)$ and $g_0(s)$ have the same number of open-loop unstable poles. Then the uncertain closed loop system is stable under unity feedback if and only if $k_N(\omega) < 1 \quad \forall \omega$.

A complete proof is given in Latchman and Crisalle (1995) and in Latchman *et al.* (1997), for the case where $\mathcal{V}_c(\omega)$ is convex. The extension of the proof to the nonconvex case is straightforward, and is omitted here for brevity. Note that $k_N(\omega)$ serves to quantify the robust stability of the closed-loop system, and it is obtained from knowledge of the critical perturbation radius $\rho_c(\omega)$. The challenging task is in fact the calculation of the critical perturbation radius.

When $\mathcal{V}_c(\omega)$ is convex, definition (2) indicates that $\rho_c(\omega)$ represents the distance between the point $g_0(s)$ and the point where the critical line intersects the boundary of $\mathcal{V}_c(\omega)$. On the other hand, when $\mathcal{V}_c(\omega)$ is nonconvex there are multiple points where the critical line intersects

the boundary of $\mathcal{V}(\omega)$; in such cases equation (3) shows that $\rho_c(\omega)$ is a function of the distance between $g_0(s)$ and the particular boundary intersection point that is closest to the critical point $-1+j0$. Under this interpretation it follows that definition (2) is a special case of the more general definition (3). Since in many cases the convexity of $\mathcal{V}_c(\omega)$ for all frequencies may not be known *a priori* the new definition of critical radius allows the application of the critical direction theory to a more general class of uncertain systems.

The Nyquist robust stability margin $k_N(\omega)$ computed using the general definition (3) for $\rho_c(\omega)$ is attractive from an analysis standpoint because through Theorem 2.1 it gives necessary and sufficient conditions for robust stability. On the other hand, if the Nyquist robust stability margin is computed using definition (2) for $\rho_c(\omega)$, then the condition $k_N(\omega) < 1 \quad \forall \omega$ is only sufficient for robust stability when $\mathcal{V}_c(\omega)$ is nonconvex. From a synthesis standpoint, assuming convexity of the critical value sets may result in more conservative controllers, the price paid for reducing the complexity of the computations. It must be remarked, however, that when $\mathcal{V}_c(\omega)$ is in fact convex, using definition (2) for $\rho_c(\omega)$ makes $k_N(\omega) < 1 \quad \forall \omega$ a necessary and sufficient condition for robust stability; hence, in such cases controllers designed using this definition are not conservative. It is the observation of the authors that in most practical problems the critical value sets are indeed convex. It must also be emphasized that the uncertainty value set $\mathcal{V}(\omega)$ itself does not have to be convex for the critical uncertainty value set $\mathcal{V}_c(\omega)$ to be convex. Therefore, from a practical point of view the less complex definition (2) for $\rho_c(\omega)$ is appropriate for design, even though there may be some conservatism when the uncertainty induces nonconvex critical value sets.

3. Affine Uncertainty Structure and Value Set Properties

The generalized critical direction theory presented in the previous section can be applied to systems with the structure

$$g(s, q) = \frac{n_0(s) + \sum_{i=1}^p q_i n_i(s)}{d_0(s) + \sum_{i=1}^p q_i d_i(s)}, \quad q \in \mathcal{Q} \quad (4)$$

where $n_0(s)$ and $d_0(s)$ are nominal polynomials, $n_i(s)$ and $d_i(s)$ are perturbation polynomials, and $q = [q_1, q_2, \dots, q_p]^T$ is the perturbation parameter vector belonging to the bounded rectangular polytope

$$\mathcal{Q} = \left\{ q \in \mathbb{R}^p \mid q_i^- \leq q_i \leq q_i^+, i = 1, 2, \dots, p \right\}$$

Clearly, (4) defines a class of finite dimensional, linear, time-invariant, real, and affine parametric uncertainties.

Fu (1990) presents two useful properties of the uncertainty value sets generated by systems with this

uncertainty structure: (i) the boundary $\partial\mathcal{V}(\omega)$ of the uncertainty value set $\mathcal{V}(\omega)$ at each fixed frequency is mapped by the edges of \mathcal{Q} , and (ii) the image on the Nyquist plane of each edge of \mathcal{Q} is either a circular arc or a line segment that can easily be calculated analytically.

4. Computation of the Critical Perturbation Radius

The computation of the Nyquist robust stability margin $k_N(\omega)$ requires that the critical perturbation radius $\rho_c(\omega)$ be calculated first. This requires finding the point of intersection of the critical line with the point on the boundary of the value set that is closest to the critical point. The calculation must be carried out at each frequency. For the case of affine-uncertain systems of the form (4), the intersection point in question can be identified using an effective strategy consisting of two steps. Let $\partial\mathcal{V}(\omega)$ represent the boundary of the uncertainty value set $\mathcal{V}(\omega)$ and $E(\mathcal{Q})$ represent the edges of the polytope \mathcal{Q} . The first step consists of finding the set of points $I = \{ \mathcal{P}_n(j\omega), n = 1, 2, \dots, k \}$ that correspond to intersections of the critical-direction ray $r(\omega)$ with $g(j\omega, E(\mathcal{Q}))$ (i.e., the image of the edges of \mathcal{Q}). This reduces to a simple problem in computational geometry after recognizing that Fu's work shows that $g(j\omega, E(\mathcal{Q}))$ is a collection of circular arcs and straight-line segments. Further details are given in Section 4.1. Note that all the points in I are elements of $\mathcal{V}_c(\omega)$ because each point in turn belongs to $r(\omega)$; however, some of these points are not necessarily elements of $\partial\mathcal{V}(\omega)$.

The second step consists of selecting one point $\mathcal{P}_c(j\omega)$ from the set of intersections I such that (i) $\mathcal{P}_c(j\omega)$ belongs to $\partial\mathcal{V}(\omega)$, and (ii) $\mathcal{P}_c(j\omega)$ is closest to the critical point $-1+j0$. When $\mathcal{V}_c(\omega)$ is convex it is straightforward to conclude that $\mathcal{P}_c(j\omega)$ is simply the point in I that is farthest away from the nominal point $g_0(j\omega)$ because, due to convexity, this is in fact the only element of I that is also an element of $\partial\mathcal{V}(\omega)$. This satisfies requirements (i) and (ii). On the other hand, when $\mathcal{V}_c(\omega)$ is nonconvex, the procedure is slightly more complicated since two cases must be differentiated depending on whether $-1+j0 \notin \mathcal{V}_c(\omega)$ (case 1) or $-1+j0 \in \mathcal{V}_c(\omega)$ (case 2). Case 1 is the simplest since $\mathcal{P}_c(j\omega)$ is naturally the point in I that is closest to the critical point $-1+j0$. This point satisfies requirements (i) and (ii) because when $-1+j0$ is not in $\mathcal{V}_c(\omega)$ the point on I that is closest to $-1+j0$ is necessarily on $\partial\mathcal{V}(\omega)$. Case 2 is a somewhat more subtle case, but nevertheless still fairly straightforward. Without loss of generality, let's assume that the points in I are ordered in increasing distance from the nominal point, and that $\mathcal{P}_1(j\omega)$ and $\mathcal{P}_k(j\omega)$ are respectively the closest and farthest points from $g_0(j\omega)$. Now consider successively all the straight-line segments $\mathcal{P}_n \mathcal{P}_{n+1}$, $n = 1, 2, \dots, k-1$, defined by adjacent intersections points $\mathcal{P}_n(j\omega)$ and $\mathcal{P}_{n+1}(j\omega)$, and identify the set P consisting of all the

points $\varphi_n(j\omega)$ and $\varphi_{n+1}(j\omega)$ that define segments whose midpoints lie outside $\mathcal{V}_c(\omega)$ (these are of course those segments whose points are outside $\mathcal{V}_c(\omega)$) except for the end-points $\varphi_n(j\omega)$ and $\varphi_{n+1}(j\omega)$ which are necessarily elements of $\partial\mathcal{V}(\omega)$. Finally, define $\varphi_c(j\omega)$ as the element of I' that is closest to the critical point $-1+j0$. Clearly, this point satisfies requirements (i) and (ii), and thus the method successfully identifies the point sought. Note that the procedure discussed in this paragraph requires a method for determining if $-1+j0 \in \mathcal{V}_c(\omega)$; furthermore, case 2 also requires determining if the midpoint of a segment on the Nyquist plane lies on $\mathcal{V}_c(\omega)$. This problem is solved in Section 4.2 where a test is presented to determine whether a given point on the Nyquist plane is an element of $\mathcal{V}_c(\omega)$.

4.1. Intersection of a Ray and Arcs in the Complex Plane

The basic geometric objects of interest are lines, circles, rays and arcs. A line passing through two points $p_0, p_1 \in \mathbb{C}$ can be represented by

$$L(p_0, p_1) := \{z \in \mathbb{C} \mid z = p_0 + t(p_1 - p_0), t \in \mathbb{R}\} \quad (5)$$

The same relation can be used to represent a ray, $r(p_0, p_1)$ with origin at p_0 and pointing towards p_1 by restricting the parameter t to non-negative values. A circle with center at z_0 and radius r_0 satisfies the relation

$$C(z_0, r_0) := \{z \in \mathbb{C} \mid \overline{(z - z_0)}(z - z_0) = r_0^2\} \quad (6)$$

where $r_0 \in \mathbb{R}^+$ and $\mathbb{R}^+ := \{x \in \mathbb{R} \mid x > 0\}$. Therefore, two parameters are sufficient to define a circle. On the other hand, three parameters are required for an oriented arc that passes through the three points $a_0, a_1, a_2 \in \mathbb{C}$, in that order, and will be described implicitly by the ordered triplet $a(a_0, a_1, a_2)$.

The cross product of two vectors is useful in determining the relative positions of points and the orientation of rays and arcs in the plane (Cormen *et al.*, 1990). Let $p_0, p_1 \in \mathbb{C}$. The cross product of p_0 and p_1 can then be defined as

$$p_0 \times p_1 := \text{Im}\{\overline{p_0} p_1\}$$

The sign of the cross product determines the relative orientation of p_0 and p_1 with respect to the origin: p_1 lies to the left of p_0 if $p_0 \times p_1 < 0$, p_1 lies to the right of p_0 if $p_0 \times p_1 > 0$, and p_1 and p_0 are collinear if $p_0 \times p_1 = 0$. The cross product can also be used to determine the direction in which a circular arc "turns". Let $a(a_0, a_1, a_2)$ be an ordered triplet defining a circular arc that starts at a_0 , passes through a_1 , and ends at a_2 . Then, the arc turns left (right) if $(a_2 - a_0) \times (a_1 - a_0) > 0$ (< 0). If $(a_2 - a_0) \times (a_1 - a_0) = 0$ then the three points are collinear and the arc degenerates into a line segment. The arc $a(a_0, a_1, a_2)$ is said to be positive (negative) if it turns left (right).

The following three-step strategy to compute the intersection of a ray and a finite number of arcs is proposed: (i) find $I = L \cap C$, the intersections (if any) of the supporting line (*i.e.*, the line that contains the ray) and the supporting circles (*i.e.*, the circles that contain the arcs), (ii) find $I_r = r \cap I$, the intersections of the ray and the supporting circles, and (iii) find $I_{ar} = a \cap I_r$, the intersections of the ray and the arcs. Consider a ray $r(p_0, p_1)$ and an arc $a(a_0, a_1, a_2)$ with supporting line $L(p_0, p_1)$ and supporting circle $C(z_0, r)$ given by (5) and (6), respectively. The intersection of the supporting line and circle, I , is determined by the real solutions of the quadratic equation $at^2 + bt + c = 0$, where

$$\begin{aligned} a &= |p_1 - p_0|^2 \\ b &= 2 \text{Re}\left\{\overline{(p_1 - p_0)}(p_0 - z_0)\right\} \\ c &= |p_0|^2 + |z_0|^2 - \left(r^2 + 2 \text{Re}\left\{\overline{p_0} z_0\right\}\right) \end{aligned}$$

It readily follows that there are no intersections if the discriminant $d = b^2 - 4ac$ is negative. Furthermore, if the determinant is zero the line is tangent to the circle and there is only one intersection. Finally, there are two intersections when the discriminant is positive. Let $\{t_i\}$, $i = 1, 2$ denote the real solutions to the quadratic equation for the case where the discriminant is positive. To find $I_r \subset I$, it is sufficient to discard the points that correspond to negative values of t_i . Finally, $I_{ar} \subset I_r$ can be determined using the cross product. Consider an arc $a(a_0, a_1, a_2)$ and the potential intersection points $I_r = \{w_1, w_2\}$. Then w_i belongs to I_{ar} if and only if the arcs $a(a_0, a_1, a_2)$ and $a(a_0, w_i, a_2)$ are both positive or both negative (*i.e.*, they turn in the same direction). In the implementation of this algorithm care should be taken to consider all degenerate cases; the details are omitted here for brevity.

4.2. Uncertainty Value Set Membership

The uncertain system given in (4) with affine parametric uncertainty can be represented in the vector-matrix form

$$\begin{aligned} g(s, q) &= \begin{bmatrix} 1 \\ s \\ \vdots \\ s^m \end{bmatrix}^T \left(\begin{bmatrix} n_{00} \\ n_{10} \\ \vdots \\ n_{m0} \end{bmatrix} + \begin{bmatrix} n_{01} & n_{02} & \cdots & n_{0p} \\ n_{11} & n_{12} & \cdots & n_{1p} \\ \vdots & \vdots & \ddots & \vdots \\ n_{m1} & n_{m2} & \cdots & n_{mp} \end{bmatrix} \begin{bmatrix} q_1 \\ q_2 \\ \vdots \\ q_p \end{bmatrix} \right) \\ &= \begin{bmatrix} 1 \\ s \\ \vdots \\ s^n \end{bmatrix}^T \left(\begin{bmatrix} d_{00} \\ d_{10} \\ \vdots \\ d_{n0} \end{bmatrix} + \begin{bmatrix} d_{01} & d_{02} & \cdots & d_{0p} \\ d_{11} & d_{12} & \cdots & d_{1p} \\ \vdots & \vdots & \ddots & \vdots \\ d_{n1} & d_{n2} & \cdots & d_{np} \end{bmatrix} \begin{bmatrix} q_1 \\ q_2 \\ \vdots \\ q_p \end{bmatrix} \right) \quad (7) \\ &= \frac{s_n^T (n_0 + N_p q)}{s_d^T (d_0 + D_p q)} \end{aligned}$$

where s_n and s_d are vectors of length $m+1$ and $n+1$, respectively, containing powers of the Laplace variable s ,

and where $n_0 \in \mathbb{R}^{m+1}$, $d_0 \in \mathbb{R}^{n+1}$, $N_p \in \mathbb{R}^{(m+1) \times (p)}$ and $D_p \in \mathbb{R}^{(n+1) \times (p)}$ are constants that represent the structure of the affine parametric uncertainty. The Nyquist image $g(j\omega, q)$ of (7) is obtained by evaluating the vectors s_n and s_d at $s = j\omega$ to yield

$$s_{n,\omega}^T = [1 \quad j\omega \quad -\omega^2 \quad -j\omega^3 \quad \omega^4 \quad \dots]$$

$$s_{d,\omega}^T = [1 \quad j\omega \quad -\omega^2 \quad -j\omega^3 \quad \omega^4 \quad \dots]$$

Now the vectors $s_{n,\omega}$ and $s_{d,\omega}$, which are constants for a particular ω , and n_0 , N_p , d_0 and D_p can be separated into real and imaginary parts. Consider the definitions

$$s_{n,R}^T = [1 \quad -\omega^2 \quad \omega^4 \quad -\omega^6 \quad \dots]$$

$$s_{n,I}^T = [\omega \quad -\omega^3 \quad \omega^5 \quad -\omega^7 \quad \dots]$$

$$s_{d,R}^T = [1 \quad -\omega^2 \quad \omega^4 \quad -\omega^6 \quad \dots]$$

$$s_{d,I}^T = [\omega \quad -\omega^3 \quad \omega^5 \quad -\omega^7 \quad \dots]$$

and

$$n_{0,R} = \begin{bmatrix} n_{00} \\ n_{20} \\ \vdots \end{bmatrix} \in \mathbb{R}^{\lceil m/2 \rceil + 1}, \quad n_{0,I} = \begin{bmatrix} n_{10} \\ n_{30} \\ \vdots \end{bmatrix} \in \mathbb{R}^{\lceil (m+1)/2 \rceil}$$

$$N_{p,R} = \begin{bmatrix} n_{01} & n_{02} & \dots & n_{0p} \\ n_{21} & n_{22} & \dots & n_{2p} \\ \vdots & \vdots & \dots & \vdots \end{bmatrix} \in \mathbb{R}^{\lceil m/2 \rceil + 1 \times p}$$

$$N_{p,I} = \begin{bmatrix} n_{11} & n_{12} & \dots & n_{1p} \\ n_{31} & n_{32} & \dots & n_{3p} \\ \vdots & \vdots & \dots & \vdots \end{bmatrix} \in \mathbb{R}^{\lceil (m+1)/2 \rceil \times p}$$

$$d_{0,R} = \begin{bmatrix} d_{00} \\ d_{20} \\ \vdots \end{bmatrix} \in \mathbb{R}^{\lceil n/2 \rceil + 1}, \quad d_{0,I} = \begin{bmatrix} d_{10} \\ d_{30} \\ \vdots \end{bmatrix} \in \mathbb{R}^{\lceil (n+1)/2 \rceil}$$

$$D_{p,R} = \begin{bmatrix} d_{01} & d_{02} & \dots & d_{0p} \\ d_{21} & d_{22} & \dots & d_{2p} \\ \vdots & \vdots & \dots & \vdots \end{bmatrix} \in \mathbb{R}^{\lceil n/2 \rceil + 1 \times p}$$

$$D_{p,I} = \begin{bmatrix} d_{11} & d_{12} & \dots & d_{1p} \\ d_{31} & d_{32} & \dots & d_{3p} \\ \vdots & \vdots & \dots & \vdots \end{bmatrix} \in \mathbb{R}^{\lceil (n+1)/2 \rceil \times p}$$

where $\lceil \cdot \rceil$ represents the greatest integer function. Using this notation the uncertain system becomes

$$g(j\omega, q) = \frac{s_{n,R}^T(n_{0,R} + N_{p,R}q) + js_{n,I}^T(n_{0,I} + N_{p,I}q)}{s_{d,R}^T(d_{0,R} + D_{p,R}q) + js_{d,I}^T(d_{0,I} + D_{p,I}q)}$$

Now consider a point $w = w_R + jw_I \in \mathbb{C}$ with finite magnitude. To determine if the point w is a member of the value set $\mathcal{V}(\omega)$ for a particular frequency, it must be determined if there is a vector $q \in Q$ such that $g(j\omega, q) = w$. Using the previous notation this is equivalent to solving the equation

$$s_{n,R}^T(n_{0,R} + N_{p,R}q) + js_{n,I}^T(n_{0,I} + N_{p,I}q) = [s_{d,R}^T(d_{0,R} + D_{p,R}q) + js_{d,I}^T(d_{0,I} + D_{p,I}q)](w_R + jw_I)$$

Equating the real and imaginary parts and rearranging terms yields

$$\begin{bmatrix} s_{n,R}^T N_{p,R} - w_R s_{d,R}^T D_{p,R} + w_I s_{d,I}^T D_{p,I} \\ s_{n,I}^T N_{p,I} - w_R s_{d,I}^T D_{p,I} - w_I s_{d,R}^T D_{p,R} \end{bmatrix} q = \begin{bmatrix} -s_{n,R}^T n_{0,R} + w_R s_{d,R}^T d_{0,R} - w_I s_{d,I}^T d_{0,I} \\ -s_{n,I}^T n_{0,I} + w_R s_{d,I}^T d_{0,I} + w_I s_{d,R}^T d_{0,R} \end{bmatrix} \quad (8)$$

which is of the form

$$A(w)q = b(w) \quad (9)$$

where the real matrix $A(w) \in \mathbb{R}^{2 \times p}$ and the real vector $b(w) \in \mathbb{R}^2$ are dependent on the uncertainty structure and the particular point w . The latter equation is a system of two linear equations with an unknown vector q . The solution represents all the points q in the parameter space that map under $g(j\omega, q)$ to a point w in the complex plane. Therefore, to determine if an arbitrary point $w \in \mathbb{C}$ is a member of the value set, it suffices to determine if there exists a solution $q \in Q$ to equation (9). This is a standard linear equality/inequality feasibility problem of the form: does there exist $q \in \mathbb{R}^p$ that satisfies equation (9) subject to the constraints

$$\begin{bmatrix} 1 & 0 & 0 & \dots \\ -1 & 0 & 0 & \dots \\ 0 & 1 & 0 & \dots \\ 0 & -1 & 0 & \dots \\ \vdots & \dots & \dots & \vdots \\ \vdots & \dots & \dots & \vdots \\ 0 & \dots & 0 & 1 \\ 0 & \dots & 0 & -1 \end{bmatrix} q \leq \begin{bmatrix} q_1^+ \\ q_1^- \\ q_2^+ \\ q_2^- \\ \vdots \\ \vdots \\ q_p^+ \\ q_p^- \end{bmatrix}$$

The solution can be found in many linear programming references (see Luenberger, 1984, for example).

5. Example

Consider the uncertain system

$$p(s, q) = \frac{s^2 + (4 + 0.4q_1 + 0.2q_2)s + (20 + q_1 - q_3)}{d(s, q)} \quad (10)$$

where

$$d(s, q) = s^4 + (9.5 + 0.5q_1 - 0.5q_2 + 0.5q_3)s^3 + (27 + 2q_1 + q_2)s^2 + (22.5 - q_1 + q_3)s + 0.1$$

and

$$(q_1, q_2, q_3) \in Q = \{(q_1, q_2, q_3) \mid -3 \leq q_i \leq 3, i = 1, 2, 3\}$$

System (10) is a modified version of the model investigated by Fu (1990). Note that the transfer function coefficients depend affinely on the parameters $q \in Q$. The goal is to analyze the robustness of the proportional-derivative controller $c(s) = 0.3s + 1$.

The system $g(s, q) = p(s, q)c(s)$ can be written in the form (7). The nominal plant $g_0(s) = g(s, q_0)$ is obtained with $q_0 = (0, 0, 0)$. For this particular system, the Nyquist robust stability margin $k_N(\omega)$ and the critical perturbation radius $\rho_c(\omega)$ can be calculated for any frequency using the method described in Section 4. Theorem 2.1 can now be employed to assess the robust stability of the system under unity negative feedback. This requires that $k_N(\omega) = \rho_c(\omega) / |1 + g_0(j\omega)|$ be less than 1 for all frequency. Note that it is not feasible to calculate $\rho_c(\omega)$ for all frequencies. Instead, $\rho_c(\omega)$ is determined for a sufficiently large number of frequencies. For this example, $\rho_c(\omega)$ and $k_N(\omega)$ are calculated for a sequence of 100 frequency points equally spaced in a logarithmic scale in the range $[0.001, 10]$. The results are shown in Figure 3 and Figure 4. From Figure 4 it is readily concluded that $k_N(\omega) < 1 \forall \omega > 0$. Therefore, the system is robustly stable for the given controller.

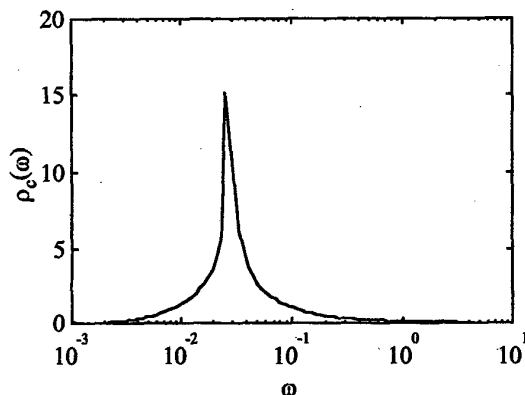


Figure 3. Critical perturbation radius $\rho_c(\omega)$ for the example.

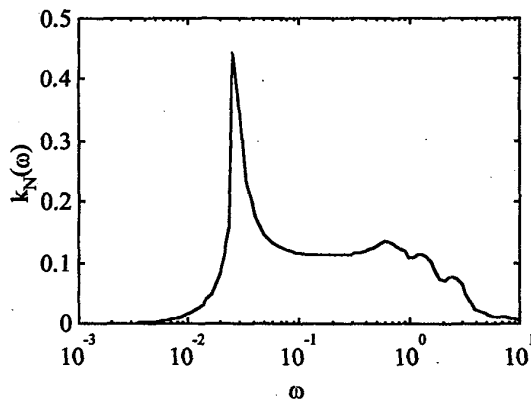


Figure 4. Nyquist robust stability margin $k_N(\omega)$ for the example.

6. Conclusion

The Nyquist robust stability margin $k_N(\omega)$ is an effective scalar measure of robust stability. The key advance is the introduction of a general definition of the critical perturbation radius $\rho_c(\omega)$ that can account for nonconvex critical uncertainty value sets. This generalization of the critical direction theory is illustrated for systems with affine parametric uncertainty for which the critical perturbation radius can be calculated precisely and efficiently with no computational issues. The calculations involve straightforward planar geometry operations and the solving of simple linear equality/inequality feasibility problems.

Acknowledgments

The first and last authors gratefully acknowledge support received from the National Science Foundation under grant number CTS 9502936.

References

- Barmish, B. R. (1992). "Extreme point results for robust stabilization of interval plants with first order compensators," *IEEE Trans. AC*, Vol. 37, pp. 707-715.
- Bartlett, A. C., Tesi, A., and Vicino, A. (1990). "Frequency response of uncertain systems with interval plants," *IEEE Trans. AC*, Vol. 38, pp. 929-933.
- Chapellat, H. and Bhattacharyya, S. P. (1989). "A generalization of Kharitonov's theorem: Robust stability of interval plants," *IEEE Trans. AC*, Vol. 34, pp. 1100-1108.
- Cormen, T., Leiserson, C., and Rivest, R. (1990). *Introduction to Algorithms*. McGraw Hill.
- Doyle, J. (1982). "Analysis of feedback systems with structured uncertainties," *IEE Proc. Pt. D.*, 129, pp. 242-250.
- Fu, M. (1990). "Computing the frequency response of linear systems with parametric perturbations," *Systems and Control Letters*, Vol. 15, pp. 45-52.
- Kharitonov, V. L. (1979). "Asymptotic stability of an equilibrium position of a family of systems of linear differential equations," *Differential Equations*, Vol. 14, pp. 1483-1485.
- Latchman, H. A. and Crisalle, O. D. (1995). "Exact robustness analysis for highly structured frequency-domain uncertainties," *Proc. ACC*, pp. 3982-3987, Seattle, WA.
- Latchman, H. A., Crisalle, O. D., and Basker, V. R. (1997). "The Nyquist robust stability margin - A new metric for robust stability," *International J. of Robust and Nonlinear Control*, Vol. 7, pp. 211-226.
- Luenberger, D.G. (1984). *Linear and Nonlinear Programming*. Addison-Wesley.
- Safonov, M.G. (1982). "Stability margins of diagonally perturbed multivariable feedback systems," *IEE Proc. Pt. D.*, 129, pp. 251-256.